



Chapter 5

Learning about the structure of strongly lensed AGNs from their lightcurves

Dominique Sluse 

University of Liège
STAR Institute, Quartier Agora - Allée du six Août, 19c B-4000 Liège, Belgium.
email: dsluse@uliege.be

Abstract. The lightcurves of strongly lensed AGNs get distorted due to gravitational microlensing, which differently magnifies the emission regions of AGNs depending on their size. This effect has been used to measure the size of the AGN accretion disc, but high photometric accuracy lightcurves reveal coherent variations on short time-scales that are not expected by standard accretion disc models. I show that this signal can be produced by emission from the Broad Line Region (BLR) but also by extended (diffuse) continuum emission. I explain how these features can be used to measure the size of the BLR but also reveal additional sources of emission. The multi-colour lightcurves of lensed AGNs, such as those to be obtained with the Vera Rubin Observatory, may become a powerful new tool to reveal the sub-parsec structure of AGNs, and shed light on elusive AGN emitting regions such as the one producing diffuse continuum emission.

Keywords. gravitational lensing, micro-lensing

1. Microlensing and AGN structure

The multiple images of strongly lensed active galactic nuclei (AGN) constitute powerful natural laboratories for studying the physical mechanisms at work in the direct vicinity of distant supermassive black holes. Strong lensing provides natural magnification which turns lensing galaxies into natural telescopes, giving access to fainter objects for a fixed observational setup. Because of the time delay existing between lensed images, strong lensing even works as a time-machine, providing images of the same system up to hundreds of days before/after their actual observations. In general the individual lightcurves of each lensed image do not perfectly match after correcting for the time-delay. The reason is the microlensing produced by the stars in the lensing galaxy. While the microlensing signal has been seen as a nuisance for a number of applications, such as time-delay cosmography (e.g. [Tewes et al. 2013](#)), it encodes information about the structure of the lensed AGNs on the scale of a stellar-mass Einstein radius, namely an angular scale of micro-arcseconds (i.e. $< 10^{-2}$ pc in the source plane). Since the phenomenon is dynamic, with substantial variations of microlensing amplitude taking place on timescales ranging from a few months to several years, tracking microlensing variability enables one to virtually “scan” the inner-most part of AGNs otherwise unresolved with existing observational facilities.

Because the dominant contribution to AGN emission in the near-UV/optical range arises from the power-law continuum emission, it means that most of the microlensing signal detected in optical lightcurves is caused by microlensing of the accretion disc producing that continuum. The amplitude of the microlensing signal directly scales with the size of source: the smaller the source is compared to the (microlensing) Einstein radius,

the stronger is the expected strength of the microlensing signal. This property has been used to measure the size of the accretion disc, commonly found to be larger than the prediction of the standard Shakura-Sunyaev accretion disc model. Moreover, because the disc size is more compact in the blue than in the red, the amplitude of microlensing may in general decrease with increasing wavelength. Consequently, by studying the chromatic changes of microlensing as a function of time, it becomes possible to constrain the wavelength dependence of the effective size of the disc. This method nicely complements continuum reverberation mapping of the disc, which requires very high photometric accuracy and a dense observational sampling. Compared to reverberation mapping, microlensing shines up for more distant AGNs (as strong lensing is required) and accommodates lower sampling of the light curves. For those reasons, the large synoptic survey telescope (LSST) is expected to be a fantastic tool for constraining the accretion discs of hundreds of distant lensed quasars through the analysis of their multicolor lightcurves (Neira et al. 2020).

The existing forecasts of microlensing signal as well as models of observed data display smooth (roller-coaster like) variations of the magnification as a function of time. While this effectively reproduces the main variations seen in microlensing lightcurves (obtained by taking the magnitude difference between lightcurves of pairs of lensed images after correcting for the time-delay), one often detects additional flickering beyond the noise level. This additional flickering, which appears like faster and smaller amplitude microlensing, has been identified in data already at the end of the nineties (e.g. Schild 1996; Gould & Miralda-Escudé 1997; Schechter et al. 2003), but it has received moderate attention since then. The lightcurves gathered by the COSMOGRAIL collaboration reveal that this signal is genuine, and present in many systems (e.g. Millon et al. 2020). Figure 1 shows an example of the “fast apparent microlensing” features seen in RXS J1131-1231.

The explanations for this signal fall in two categories: (a) it is caused by an unaccounted low mass (e.g. planetary-like) population of microlenses; (b) it is due to unaccounted structures in the source. In this work, we focus on the second category of explanations. In particular, we notice an important simplification when interpreting broad-band fluxes, which is that the whole flux is supposed to arise from the accretion disc. This assumption is however in general incorrect as flux from the broad emission lines is superimposed to the power-law continuum emission. This line flux often represents 30-40% of the flux in a given band, especially when iron emission is significant. Additional continuum emission arising from regions beyond the disc may not be excluded either but its reality is still debated.

In the following, we explore how emission arising from regions more extended than the continuum, and hence much less microlensed, modify the difference lightcurve between pairs of lensed images after time-shift for time-delay (hereafter generally called microlensing lightcurves). We discuss two scenarios: in the first one, we consider emission from the BLR, as originally proposed by Sluse & Tewes (2014); in the second one, we consider diffuse continuum emission (in addition to the accretion disc flux) arising from a region larger than the BLR. For both situations, we assume that the extended region reverberates the flux from the disc, with some time-lag $\tau = d/c$, where c is the speed of light and d is the distance between the continuum and the extended emission.

2. Method and main results

Our toy model emulates microlensed broad band lightcurves of AGNs with two emitting regions: a compact emission $F_{\text{cont}}(t)$ that arises exclusively from the disc and which is sufficiently compact to be microlensed, and a second component, too large to be microlensed, which responds to the continuum after a time τ . For simplicity, we assume that this extended region responds instantly to the incident continuum flux after a time τ . This

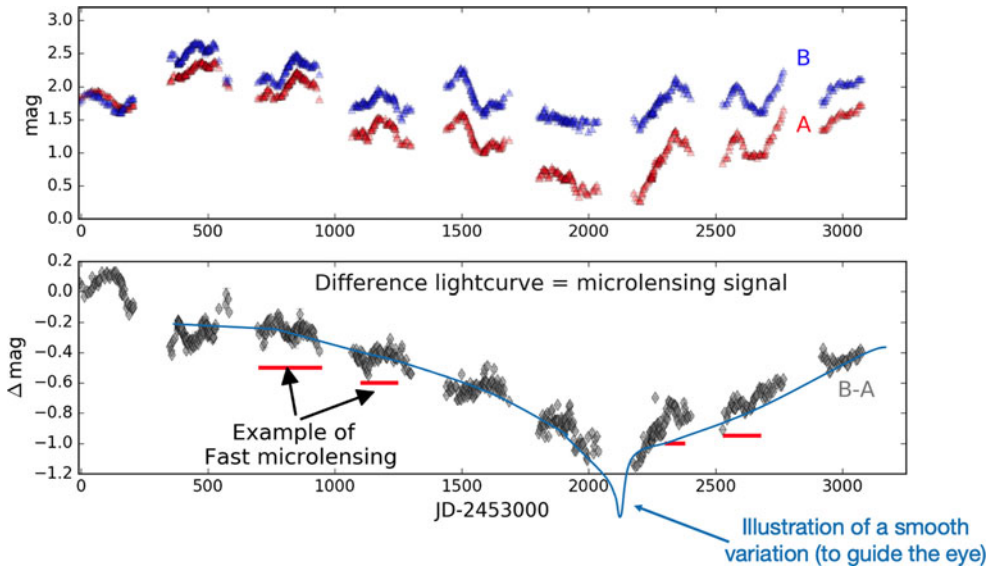


Figure 1. *Top:* Lightcurves of images A & B of the lensed AGN J1131-1231 obtained by [Tewes et al. \(2013\)](#). *Bottom:* Difference lightcurve enabling to cancel the intrinsic variability of the AGN and isolate the microlensing signal. The blue curve shows the signal (qualitative trend) that would be expected in case of microlensing of an accretion disc. The horizontal red lines indicate small amplitude “fast” variations arising on time scales of hundreds of days. Those features may be caused by structures in the source absent of existing AGN models.

academic assumption is equivalent to say that the transfer function of the reprocessing region is a Dirac $\delta(t)$ function. A more realistic situation would consist in convolving the input signal with a transfer function $\Psi(t)$, but the latter is a priori unknown. It would generally smooth out the reverberated flux. While this may have a qualitative impact on the shape of the discussed features, the general results discussed below will remain. The intrinsic variability signal $F_{\text{cont}}(t)$ of the AGN is generated using a damped random walk model, and an arbitrary microlensing magnification $\mu(t)$. To ease the interpretation, we apply microlensing to only one of the lensed images, which is equivalent to fix $\mu(t) = 1$ for the second image. The intrinsic variability signal as well as the microlensing factors are chosen to qualitatively reproduce the data of J1131-1231 displayed in Fig. 1 (Sluse et al., in prep). Ignoring the multiplicative macro-magnification of the image, we can express the observed flux F_i of the lensed image i as:

$$F_i = (1 - f) \times \mu(t) \times F_{\text{cont}}(t) + f \times F_{\text{cont}}^*(t + \tau), \tag{1}$$

where f is the fraction of flux arising from a region larger than the continuum (we assume a single region), and $F_{\text{cont}}^*(t + \tau)$ is the reverberated flux.

In our simulation, we have varied f in a range $[0.1, 0.5]$, and consider two sets of values for τ . On the one hand, we have looked at “short time-lags” with $\tau \in [10, 50]$ days, which corresponds to size of the region emitting $H\beta$ for the lens system J1131–1231. Second, we have considered the case of time lags an order of magnitude larger, namely in the range 100-500 days. This second situation corresponds to an hypothetical diffuse continuum emission emitted in the outskirts of the BLR. The details of those results will be presented in Sluse et al. (in prep) but we outline here some of our most salient findings.

Figure 2 displays the result of a simulation where $f = 0.5$ and the cases of a BLR-type lag (blue) and of a diffuse-continuum-type lag (500 days). The key features we observe are (a) the true micro-magnification is biased “proportionally” the fraction of

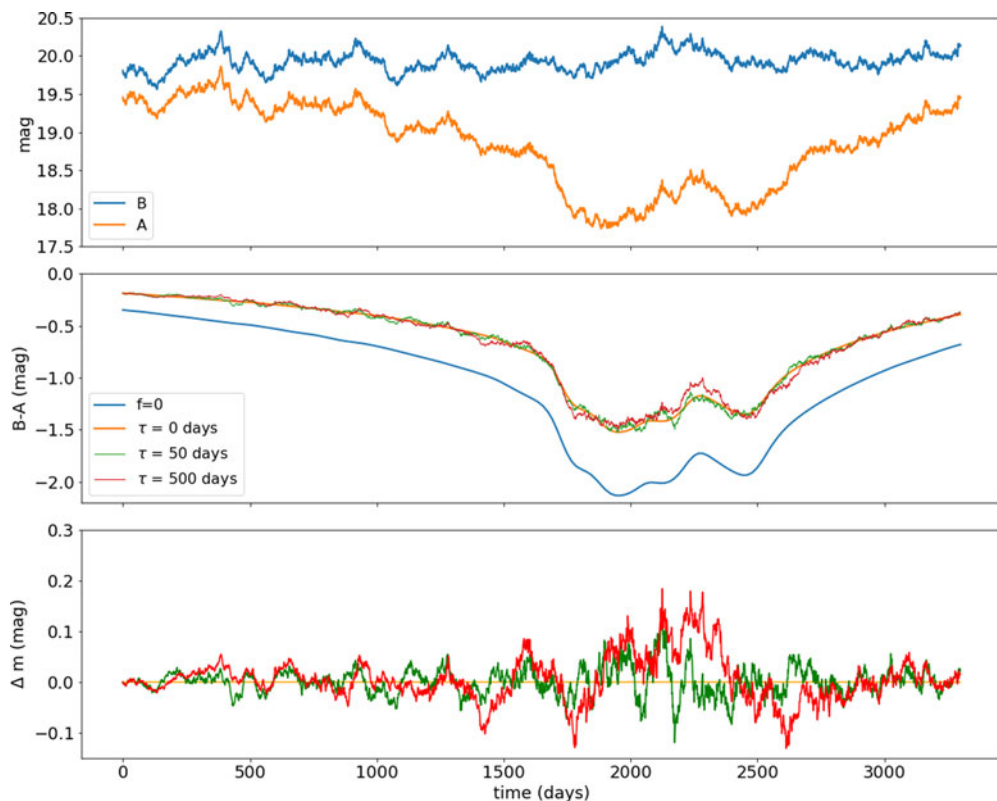


Figure 2. *Top:* Simulated broad band lightcurves of a pair of images according to Eq. 1. The panel displays a situation where $f = 0.5$, and only image A is affected by a microlensing magnification $\mu(t)$ (for an accretion-disc-like source) shown in blue in the middle panel. Fluxes have been converted to magnitude. *Middle:* Difference lightcurve $m_B - m_A$. The blue curve is for $f = 0$, while the other curves show the case where $f = 0.5$ and $\tau = 50$ days (green, BLR case), and $\tau = 500$ days (red, diffuse continuum). The orange lightcurve shows the “academic” situation where $\tau = 0$. *Bottom:* Difference between the reference ($\tau = 0$ day) and lightcurves with $\tau = 50$ days (green) and $\tau = 500$ days (red). The largest flickering is obtained when the microlensing amplitude reaches a maximum ($t \sim 2000$ – 2500 days) and $\tau = 500$ days.

non microlensed flux (the bias approximately scales with $2.5 \log(1 - f)$). (b) the amplitude of the fluctuations depends on the amplitude of intrinsic variability and of f : the larger is f , the larger is the observed fluctuation. (c) the amplitude of the fluctuation is minimum when $\mu(t)$ gets closer to 1; (d) for a fixed f , the amplitude of the fluctuation is larger for larger τ , with variation reflecting the time scale of the intrinsic variability possible over the period of the lag.

At the light of these results, we see that a flickering around the smoothly varying microlensing with an amplitude of about ± 0.1 mag may happen in our toy model for $f = 0.5$ and a time-lag larger than typically 200 days (only the 500 days lag is shown). This is in qualitative agreement with what is seen in the lightcurve of J1131–1231. As the emission from the BLR (mostly FeII) contributes only 30% of the R -band flux, it cannot explain the observed large amplitude signal. This suggests that the “fast” microlensing observed in that system could be caused by “continuum” emission arising from the outer part of the BLR or beyond. A set of spectroscopic monitoring data, not shown here, supports that finding (Sluse et al. in prep.).

3. Discussion and perspectives

There is increasing observational support for the existence of extended continuum emission in addition to the standard emission from the accretion disc, but its exact origin is yet debated (e.g. Lawrence 2012; Netzer 2022). For instance, Sluse et al. (2015); Hutsemékers et al. (2015, 2020), have shown, based on the analysis of the spectra of two Broad Absorption Line quasars, that about 40% of the UV continuum emission arises in those systems from a region more extended than the accretion disc. Diffuse continuum emission in AGNs is suspected since several decades (e.g. Korista et al. 1995; Korista & Goad 2001) but its unambiguous detection is observationally challenging. The role of diffuse emission in interpreting continuum reverberation mapping data, which are in general hardly reconciled with a Shakura-Sunyaev accretion disc model, is not completely settled (e.g. Chelouche et al. 2019; Cackett et al. 2020; Guo et al. 2022). The data from microlensed quasars as well as the simulations presented in this work show that the detailed study of microlensed AGNs may provide important clues on the existence and properties of extended continuum. High accuracy photometric monitoring of strongly lensed quasars therefore provide a new technique to study the elusive extended continuum emission present in AGNs.

The advent of LSST, providing multi-colour lightcurves for an ensemble of lensed quasars, may enable to probe the nature of this emission, offering important insights on the “mechanics” of AGNs. Several observational signatures may help identifying and characterizing the properties of any diffuse continuum emission:

- Since the fraction of BLR flux in each band can be estimated from spectroscopy, it may be possible to compare the observed amplitude of flickering to model expectations. Deviations from this prediction may indicate additional amount of continuum emission.
- Multiple lensed images provide complementary information: images strongly demagnified due to microlensing may reveal flux variations dominated by the extended continuum while large micro-magnification events will display flux dominated by the disc emission.
- The idea proposed in Sluse & Tewes (2014) of doing photometric reverberation mapping by using lightcurves of multiple lensed images can be applied to the study of diffuse continuum, but deblending the emission of any extended continuum from real BLR flux may require ancillary spectroscopic data. The use of a power spectrum analysis of the microlensed signal may also be a promising alternative to standard reverberation mapping that is based on cross-correlation between signals (Paic et al. 2022).

The addition of multi-epoch spectroscopy (even sparse) may help to break model degeneracies from multi-band LSST data (e.g. by fixing the fraction of flux from the BLR at specific epochs). Facilities such as the Wide Field Spectroscopic telescope (Ellis et al. 2017) would a great asset for this kind of work.

The promises of using microlensing to study the properties of strongly lensed AGNs may be even greater than anticipated. The analysis of hundreds of microlensed systems may enable to simultaneously probe, the properties of the accretion disc, of the BLR, but also of an overlooked ingredient: diffuse continuum emission. A revision of our detailed understanding of AGNs is on its way.

References

- Cackett, E. M., Gelbord, J., Li, Y.-R., et al. 2020, *ApJ*, 896, 1
 Chelouche, D., Pozo Nuñez, F., & Kaspi, S. 2019, *Nature Astronomy*, 3, 251
 Ellis, R. S., Bland-Hawthorn, J., Bremer, M., et al. 2017, arXiv e-prints, arXiv:1701.01976
 Gould, A. & Miralda-Escudé, J. 1997, *ApJl*, 483, L13
 Guo, H., Barth, A. J., & Wang, S. 2022, *ApJ*, 940, 20
 Hutsemékers, D., Sluse, D., Braibant, L., & Anguita, T. 2015, *A&A*, 584, A61

- Hutsemékers, D., Sluse, D., & Kumar, P. 2020, *A&A*, 633, A101
- Korista, K. T., Alloin, D., Barr, P., et al. 1995, *ApJs*, 97, 285
- Korista, K. T. & Goad, M. R. 2001, *ApJ*, 553, 695
- Lawrence, A. 2012, *MNRAS*, 423, 451
- Millon, M., Courbin, F., Bonvin, V., et al. 2020, *A&A*, 640, A105
- Neira, F., Anguita, T., & Vernardos, G. 2020, *MNRAS*, 495, 544
- Netzer, H. 2022, *MNRAS*, 509, 2637
- Paic, E., Vernardos, G., Sluse, D., et al. 2022, *A&A*, 659, A21
- Schechter, P. L., Udalski, A., Szymański, M., et al. 2003, *ApJ*, 584, 657
- Schild, R. E. 1996, *ApJ*, 464, 125
- Sluse, D. & Tewes, M. 2014, *A&A*, 571, A60
- Sluse, D., Hutsemékers, D., Anguita, T., Braibant, L., & Riaud, P. 2015, *A&A*, 582, A109
- Tewes, M., Courbin, F., Meylan, G., et al. 2013, *A&A*, 556, A22